International Journal of Engineering

Journal Homepage: www.ije.ir

Intelligent Controllers to Extract Maximum Power for 10 KW Photovoltaic System

M. Rupesh*[a], T. S. Vishwanath[b]

[a] BVRIT HYDERABAD College of Engineering for Women, Electrical & Electronics Engineering, Hyderabad, India
[b] Electronics & Communication Engineering, Bheemanna Khandre Institute of Technology Bhalki, India

A B S T R A C T

This research looks at how photovoltaic (PV) cells generate energy in different weather conditions. Photovoltaic power today plays a key role in the production of energy and satisfying the needs of consumers all over the world. The PV cell's ability to generate electricity was entirely dependent on sunshine and temperature fluctuations in the environment. Several researchers are working on a variety of MPPT methods for a photovoltaic system. Outdated MPPT techniques are unable to withstand a dramatic change in weather conditions. The fundamental purpose of this study is to associate the numerous unadventurous and clever controllers for MPPT of the PV system, such as the PSO, GA, and CNFF. The MATLAB environment was used to create and simulate the recommended intelligent controller for MPPT in the PV system. Furthermore, the aforementioned findings like Voltage, Current and Power with respect to different irradiance and temperature are compared and evaluated. The performance of the above-mentioned topologies has been related to the optimum intelligent controller for the PV system and cncluded that the CFFNN gives better efficiency with minimum time required to extract.

doi: 10.5829/ije.2022.35.04a.18

NOMENCLATURE

PV	*Photovoltaic*	f	Desired objective function
MPP	Maximum Power Point	X_i	Location of Particle
PSO	Particle Swarm Optimization	V_i	Speed of Particle
CFFNN	Cascaded Feed Forward Neural Network	w	Sluggishness weight
GA	Genetic Algorithm	r_1, r_2	Orbitory variables
N	Diode Constant	C_1, C_2	Reasoning and Common Coefficients
K	Blothzman Constant	P_{besti}	Best location of particle of i
T	Temperatre in Kelvin	Gbest	Best global location of i
Q	Electricity Charge	MG	Micro Grid
I_0	Maximum Diode Corrent	REG	Renewable Energy Generation
G	Irradiance	DG	Distribution Generation
Gref	Reference Irradiance	P & 0	Perturb and Observation
Eg	Silicon diode Band Width	INC	Incremental Conductance
D	Duty Cycle		

1. INTRODUCTION

The growing pace of population expansion and levels of urbanization are to blame for the rapid rise in energy consumption, CO_2 emissions, and worldwide demand and supply insufficiency [1-2]. Under environmental concerns such as energy shortages and pollution, renewable energy sources like solar and wind are the greatest ideal replacement energy sources, with solar and wind being the most prevalent energy in current power systems. Micro grid (MG) is a low-voltage distribution system that combines flexible DGs like wind, solar, and fuel cells with controllable storage and loads [3-6]. They increase network stability and offer long-lasting, high-

*Corresponding Author Email: m.rupesh1@gmail.com (M. Rupesh)

quality electricity. Managing an Micro Grid through a large number of Distributing Generations, variable loads, and ESA is challenging, especially given the high degree of renewable energy (REG) generating penetration. To highlight the high use of efficiency power, the REG is generally arranged using maximum power tracking (MPPT) algorithms [7-10]. As a result of the fluctuating and uncontrolled meteorological circumstances, it is classified as a generation that cannot be regulated [11-15]. Maximum power monitoring technology will be critical for getting the most energy out of a solar cell under a variety of weather situations. Regulating the solar powered non-linear current and voltage properties throughout times of low sunlight or incompletely covered conditions is a key issue. Researchers have proposed a number of MPPT techniques to obtain maximum energy output from a photovoltaic system.

P&O, Incremental Conductance and feedback power methods are among the numerous little MPPT approaches that are extremely common. Due to a lack of self-regulation capacity, the foregoing traditional approaches flop to reach the desired quickness of process and extreme power output. Various intelligent controllers based on MPPT methods are presented in this paper to attain peak power as well as operating speed (auto-adjustment). In the Matlab software, intelligence-based MPPT methods are modelled and assessed. The mathematical formulation for the solar system and the construction of the boost converter are described in section 2. Section 3 describes the different smart controllers. In section 4, the proposed smart regulators are designed and simulated in MATLAB, with the performance of the PV system evaluated under several climate situations. Section 5 concludes with the hardware and comparative investigation. The suggested research's conclusion is presented in section 6.

2. MODELING OF PV & BOOST CONVERTER

2. 1. PV System Design   The solar cell is shown as a dependent current source with extra series and parallel resistors connected to a diode in Figure 1. It's worth noting that when solar light is not there, the PV cell serves as a load and produces no power [16]. The actual current commencing the current source (PV cell) is determined by the amount of sunlight that shines on the PV cell (photo-current) (Figure 1). In an open circuit, the voltage is zero.

The Solar cell voltage generation will be affected by the voltage loss through the diode as given in Equation (1):

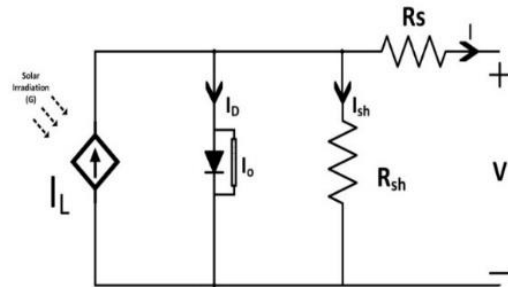$$V = \left(\frac{NKT}{Q}\right) \ln \frac{I_L - I_o}{I_o} + 1 \tag{1}$$

where

Figure 1. The Equivalent PV cell Circuit

PV Cell Open circuited Voltage = V
N stands for the diode constant 1.50
Boltz const K = $(1.381 \times 10^{-23}$ J.K$^{-1})$
T = Temperature in Kelvin
Q stands for "elementary charge" $(1.602 \times 10^{-19}$ Coulomb)
Io is the Maximum current of a diode (A)
The Generated Current by light (Radiation) is given in Equation (2).

$$I_L = \left(\frac{G}{G_{ref}}\right) * (I_{L\,ref} + \propto_{Isc} (T_C - T_{C\,ref})) \tag{2}$$

where
G = irradiation instantaneous (W/m^2)
Gref = standard Condition with reference irradiation 1000 Watts per square metre
ILref denotes a reference. Under normal circumstances, photoelectric current 0.15 A
Instant temperature Tc.
TCref stands Model temp at 298.0 K
αISC stands SC current temp co-effi (A/K)=0.0065 AK^{-1}
IL = Current Generated by the Light = Iph (A)
Output current and Reverse saturation current as Equations (3) and (4).

$$Io = I_{or} \left(\frac{T_C}{T_{ref}}\right)^3 e^{\frac{(Q*Eg)}{(K*N)*\left[\left(\frac{1}{Tcref}\right)-\left(\frac{1}{Tc}\right)\right]}} \tag{3}$$

$$I_{or} = \frac{I_{scn}}{e^{\left(\frac{V_{ocn}}{N*V_{tn}}\right)}} \tag{4}$$

where
Io = Current Capacity in Reverse
Current Capacity = Ior
Eg is the band gap of a silicon diode, which is 1.10 eV.
Current S C (Ish = Il)
Under SC circumstances, the maximum current generated by a cell: Volt = 0.00 V, which is shown in Equation (5).

$$I_{sh} = (I_L - I_0) * \left(e^{\frac{eV}{kT}} - 1\right) A \tag{5}$$

2. 2. Design of Boost Converter   This converter is a DC-DC level up converter that transforms fluctuating

DC voltage caused by weather variations to a constant stepped up voltage that may be linked to an inverter for grid integration and residential use. This converter is made up of a diode, a MOSFET, and a load ingredient to obtain the output voltage. Depending on the triggering duty cycle, the output voltage varies. The fundamental construction of a boost converter is shown in Figure 2.

The duty cycle of MOSFET can be calculated as Equation (6).

$$D = [1 - \frac{V_{in(min)} * \eta}{V_{out}}] \tag{6}$$

Change in ripple current as Equation (7):

$$di = i_{ripple} * i_{out} * \frac{v_{out}}{v_{in}} \tag{7}$$

The output current of converter as Equation (8):

$$I_{out} = \frac{Converter\ Power\ Rating}{Converter\ output\ voltage} \tag{8}$$

Inductance of boost converter as Equation (9):

$$L = \frac{[v_{in}(v_{out} - v_{in})]}{di * f_s * v_{out}} \tag{9}$$

Acceptable change in voltage as in Equation (10)

$$Dv = \frac{v_{out}}{dv\ percent/100} \tag{10}$$

Output capacitor to reduce the ripples as in Equation (11).

$$C = \frac{I_{out} * D}{f_s * dv} \tag{11}$$

Output Resistor as shown in Equation (12).

$$R = \frac{V_{out}}{I_{out}} \tag{12}$$

3. MPPT ALGORITHMS

3. 1. Particle Swarm Optimization
The movement of particles is influenced by two variables: the Pbest, which is used to save the best location of each particle as an individual best position, and the Gbest, which is discovered by comparing individual particle swarm positions [18] and saved as the best position of the

swarm. This method is used by the particle swarm to move towards the best place while continually revising its route and speed. As a result, each particle swiftly converges to an optimum or near-optimal global optimal. The equations that describe the conventional PSO technique are as follows in Equations (13) and (14).

$$V_i(k + 1) = wV_i(k) + C_1r_1(P_{best} - x_i(k)) + C_2r_2(g_{best} - x_i(k)) \tag{13}$$

$$x_i(k + 1) = x_i(k) + v_i(k + 1) \tag{14}$$

where i = 1, 2 3 . . . . .N
where xi and vi are the speed and location of particle i; k is the repetition number; w is the sluggishness weight; r1 and r2 are arbitrary variables with ideals homogeneously spread between [0,1]; and c1 and c2 are the reasoning and common coefficients. The specific best location of particle I is pbest,i, while the swarm finest location of all particles is gbest. If the initialization requirement Equation (16) was met, the technique was modified as Equation (15):

$$P_{best} = x_{ik} \tag{15}$$

$$f(x_{ik}) > f(P_{best}) \tag{16}$$

where f is the desired objective function to be maximized.
Step 1: Selection of Parameter:
For the suggested MPP procedure, the pulse width of the converter was outlined as the location of the particle, and the produced power was selected as the fitness value, assessment function. Each particle's location and preliminary speed were erratically adjusted in a identical spreading across the exploration space.
Step 2: Fitness Evaluation:

After the controller sends the duty cycle instruction, which indicates particle i's location, the fitness value of particle i is calculated.
Step 3: (Updating Distinct and Global Best Data):
By associating the afresh computed fitness values to the prior ones and substituting the pbest and gbest matching to their locations as needed, each particle's fitness values, separate best locations (Pbest), and global best fitness values (gbest) are informed.
Step 4 (Update Speed and Location of Each Particle): After analysing all particles, apprise the speeds and locations of each particle in the swarm using the PSO Equations (13) and (14).
Step 5 (Determination of Convergence): The converge criteria is either finding the best solution or completing the most iterations. The operation will end if the convergence condition is fulfilled; otherwise, repeat Steps 2 through 5.
Step 6. (Initialization):
The converge criteria in the conventional PSO technique is either finding the best solution or achieving the maximum number of repetitions. The fitness value of
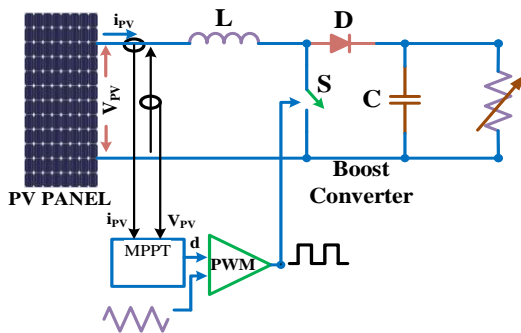

Figure 2. Boost Converter Circuit diagram

PV systems, on the other hand, is not constant since it varies depending on the weather and load.

When the PV module output changes, the PSO must be re-initialized and examine for a new MPP.When the following functions are met, the suggested PSO algorithm is reinitialized for this application using Equation (17):

$$\frac{P_i(k+1) - P_i(k)}{P_i(k)} > \Delta p \tag{17}$$

Particle swam Optimization algorithm flowchart is shown in Figure 3.

3. 2. Genetic Algorithm
The MPPT procedure, which is founded on the Genetic Algorithm (GA), is a natural genetics-inspired optimization method.

This approach, which is based on the notion of "endurance of the rightest," is used to identify an optimum set of parameters. In actuality, the search for a GA technique entails [17]. Selection, crossover, and mutation are the three basic operators. Selection is a method of choosing genetic material from the current generation's population for inclusion in the next generation's population depending on its fitness. The crossover operator connects two chromosomes to make new genetic material. The mutation operator tries to achieve some stochastic dissimilarity of GA in order to obtain quicker convergence by preserving genetic variety from one population generation to the next. To address this issue, the algorithm was tweaked to reset the initial

population whenever a change in irradiance or cell temperature is detected. As a result, if the following two requirements are fulfilled, the GA is reinitialized: Equations (18) and (19).

$$|V(k+1) - V(k)| < \Delta V \tag{18}$$

$$\left|\frac{[P_{pv}(k+1) - P_{pv}(k)]}{P_{pv}(k)}\right| > \Delta P \tag{19}$$

At iteration, the intended output voltage matches to the chromosomal location (k). Four people are applied sequentially to the starting population, which is made up of chromosomal parents. Equation (20) gives the population's initial locations.

$$[P1, P2, P3, P4] = [0.8, 0.6, 0.4, 0.2]Voc \tag{20}$$

The fitness is the produced power Ppv, which is ranked decreasingly and selected using elitism as a criteria.

To generate a kid, the crossover stage involves merging two chromosomal parents. In reality, Equations (21) and (22) are used in this phase.

$$child(k) = r\,P(r) - (1 - r)P(k + 1) \tag{21}$$

$$child(k + 1) = (r - 1)\,P(k) - (r)P(k + 1) \tag{22}$$

where r is an arbitrary integer. Equation (23). shows the relationship between the ISSBC's output voltage and duty cycle.

$$a(k) = child(k)/V \tag{23}$$

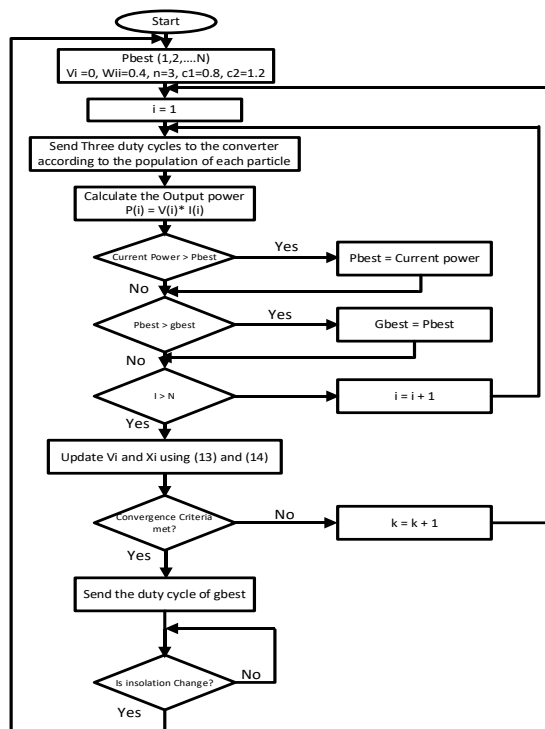Genetic algorithm flowchart is shown in Figure 4.
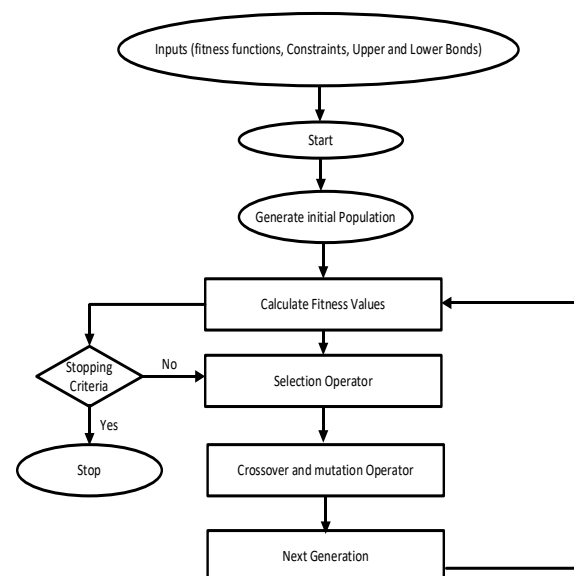
3. 3. Cascaded Feed Forward Neural Network Method
The CFNN is a feed-forward (FF) neural network with a connection from the influence layer and individually preceding layer to the subsequent layers.

Figure 3. PSO Algorithm flowchart

Figure 4. Genetic Algorithm Flowchart

The production layer is also publicly connected with the influence layer head-to-head to the hidden layer in a three-layer network. With enough hidden neurons, a cascading network with two or more layers, like FF networks, may learn any arbitrarily limited I-O connection [19-25]. The CFNN can be used for any kind of contribution to cartography creation.

The advantage of this method is that, it accounts for the non-linear relationship between entry and departure deprived of removing the linear association in the middle of the two.

The meeting created between the contribution and the production in a perceptron is a kind of unswerving connotation, however the meeting shaped in the middle of the influence and the invention in an FFNN is a subordinate connotation. An activation function in the hidden layer makes the connection non-linear. When the perceptron and multilayer grid connecting forms are merged, the grid is moulded through a straight link between the influence layer and the production layer, as well as the connection parenthetically. The CFNN is the network that results from this connecting model.

A cascading neural network is the network shaped by this linking paradigm (CFNN). The following are some examples of Equation (24):

$$y = \sum_{i=1}^{n} f^i w_i^i x_i + f^o(\sum_{j=1}^{k} w_j^o f_j^h(\sum_{i=1}^{n} w_{ji}^h x_i)) \quad (24)$$

where wii is the weight from the influence layer to the invention layer and fi is the activation function. If a bias is applied to the influence layer, and each neuron in the hidden layer has an activation function of fh, the equation becomes as Equation (25):

$$y = \sum_{i=1}^{n} f^i w_i^i x_i + f^o(w^b + \sum_{j=1}^{k} w_j^o f_j^h(w^b + \sum_{i=1}^{n} w_{ji}^h x_i)) \quad (25)$$

The CFNN model is used to analyse time series data in this study. Thus, the delays of time series data Xt-1, Xt-2, ..., Xt-p are represented by the neurons in the contribution layer, and the production is represented by the current data Xt.

As shown in Figure 5, the suggested multi-layered cataract neural network model was created for a procedure to trace extreme power spots for the PV arrangement. PV voltage and current are two of the contributions to this network. The gate pulse of the DC-DC converter is the source of this network's production. From the influence layer to the invention layer, there are four hidden layers. Each hidden layer uses a different number of neurons, for example, layer 1 uses 20 neurons, layer 2 uses 30 neurons, layer 3 uses 20 neurons, and layer 4 uses 5 neurons, as illustrated in Figure 5a. More than 10,000 data points, such as PV voltage, PV current, and gate pulse, were used to train the proposed network. The MPPT algorithm was created after more than 1000 epochs were completed, and the network was well-trained. As demonstrated in Figure 5b, the optimum

dynamic presentation of the suggested CNFF is 9.2922 x 10^{-17}. Figure 5c shows the pitch examination, Mu, and authentication patterned for the planned CNFF. Finally, in Figure 5d, the planned system regression value is shown.

4. SIMULATION RESULTS

The discovery of the Maximum Power Point utilizing several methods has been implemented in this work, and the outcomes are presented in Figure 6.
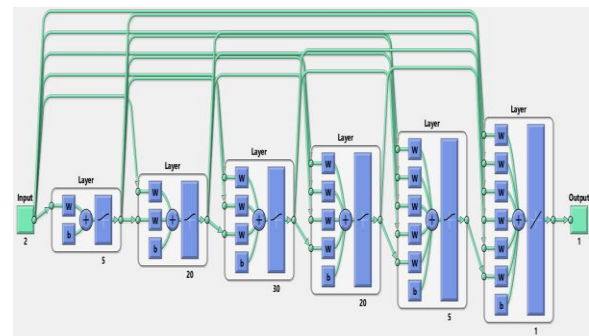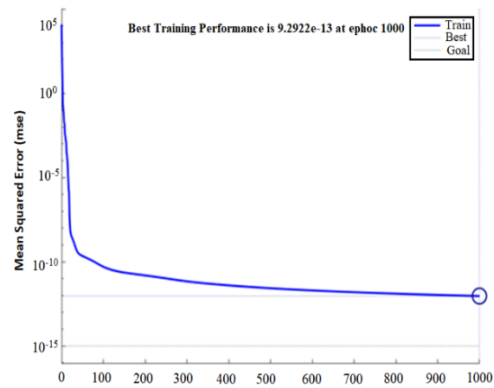

Figure 5a. CFFNN structure for MPPT Algorithm

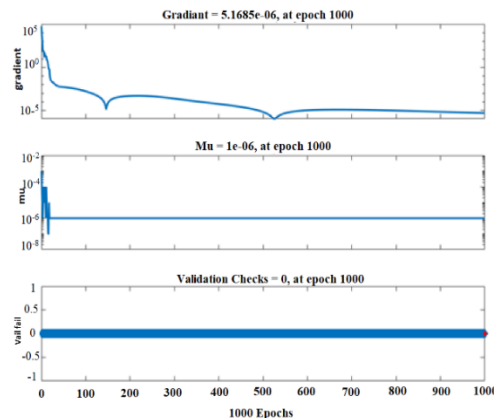**Figure 5b.** Optimum dynamic presentation of CFFNN

Figure 5c. Gradient, Mu and Authentication check for anticipated CNFF
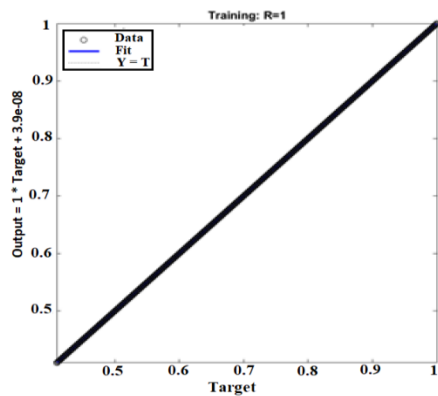
Figure 5d. Regression for suggested CNFF

4. 1. Particle Swarm Optimisation (PSO) The proposed PSO technique was applied in a 10 kW PV system MATLAB/Simulink model. Under typical operating settings, this simulation model was examined. The simulation's outcomes are assessed. Adjustable irradiance has been added to the contribution of a PV model to assess the enactment of arrangement using the same simulation model. The PV produced power and MPPT power have been measured and displayed in Figure 7a under several weather conditions. Figure 7b shows the boost converter voltage and current waveforms under various climate circumstances, 494.5 V and 19.78 V, respectively. Figure 7c shows PV voltage 308 V and Boost converter voltage 494.4 V under varied irradiance conditions.

4. 2. Genetic Algorithm (GA) As illustrated in Figure 6, the proposed GA Organizer was employed in a MATLAB/Simulink model for 10 kW rating. Under typical operating settings, this simulation model was examined. The simulation's outcomes are assessed. The changing irradiance input of the PV system has been used to the same simulation model, which analyses system performance. The PV power and MPPT power of 9743 W were measured and schemed in Figure 8a. under
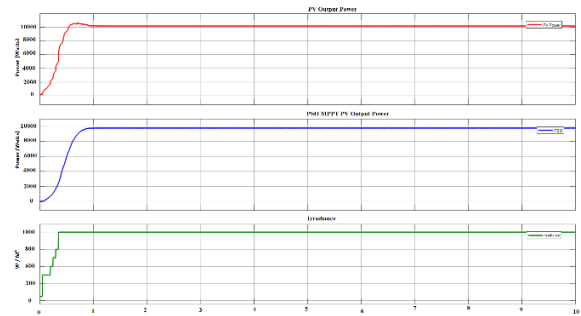

Figure 6. Simulation of 10 kW PV model for all MPPT Techniques

Figure 7a. PV power vs MPPT power under several irradiations

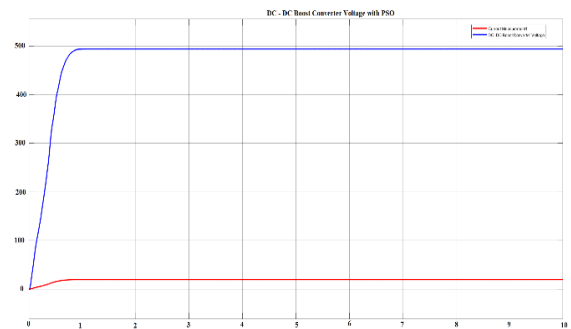**Figure 7b.** Boost converter voltage and current
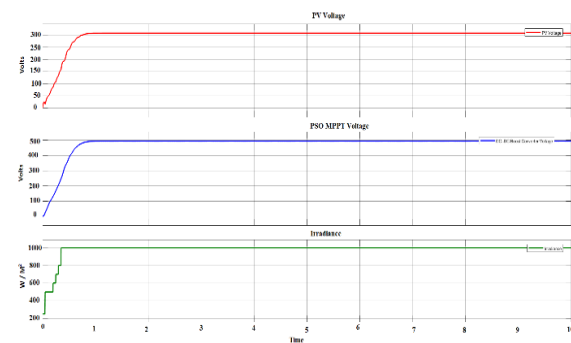
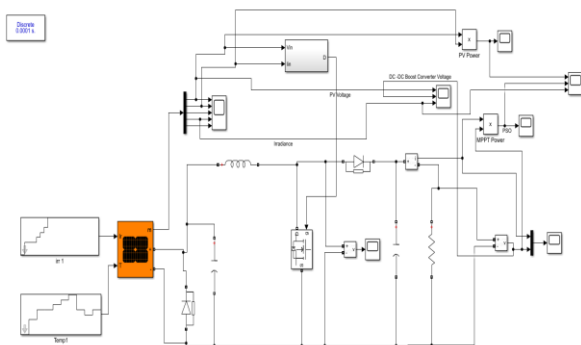**Figure 7c.** PV Voltage vs Boost converter Voltage under several irradiance

various weather conditions. Under various weather conditions, the boost converter voltage and current waveforms are shown. Figure 8b shows 491 V and 19.8 correspondingly. Under different irradiance a, relate PV voltage 310 V and Boost converter voltage 491 V. are shown in Figure 8c.

4. 3. Cascaded Feed Forword Neural Network Method As illustrated in Figure 6, the suggested CNFF Controller was executed in a MATLAB/Simulink model of a 10 KW rating. Under typical operating settings, this simulation model was examined. The simulation's outcomes are assessed. The changing irradiance input of the PV system has been used to the
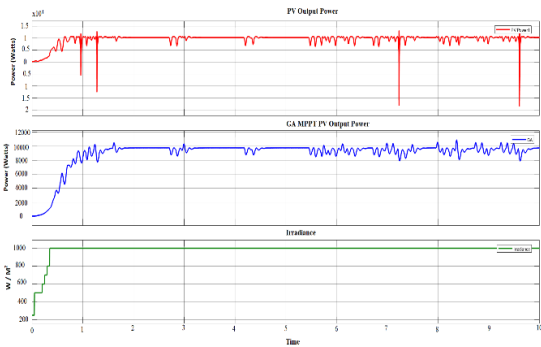
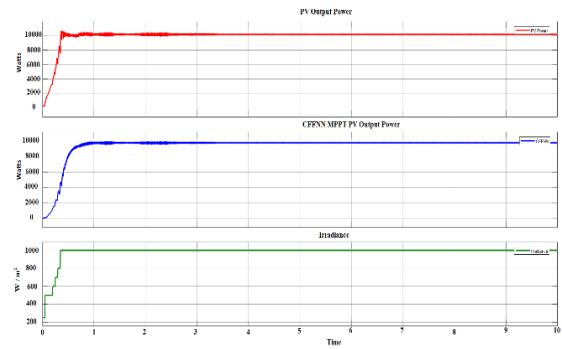**Figure 8a.** PV power vs MPPT power under various irradiance

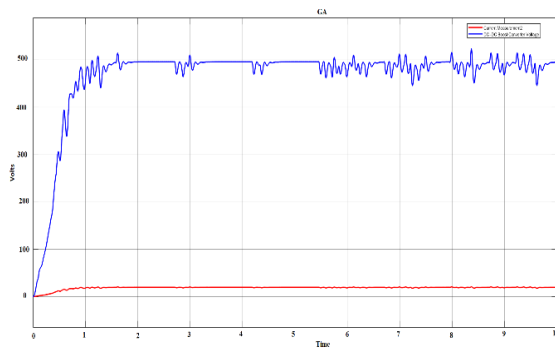**Figure 9a.** PV power vs MPPT power under various irradiation

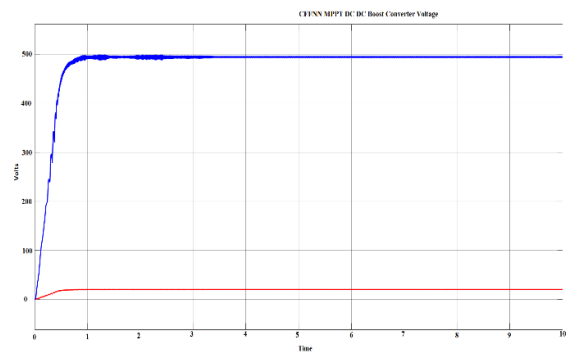**Figure 8b.** Boost converter voltage and current

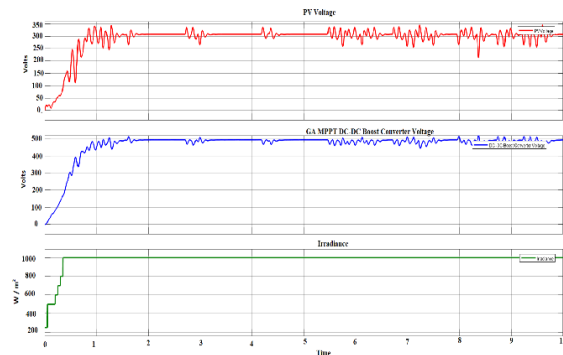**Figure 9b.** Boost converter voltage and current

Figure 8c. PV Voltage vs Boost converter voltage under various irradiance
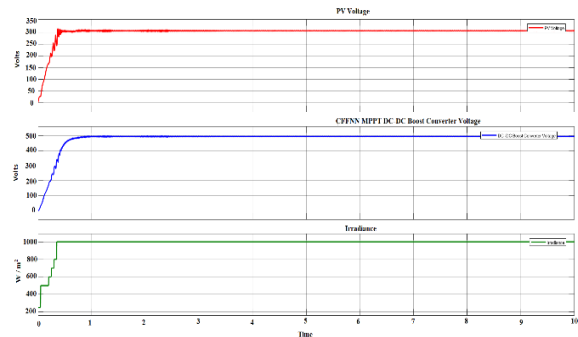

Figure 9c. PV Voltage vs Boost converter voltage under several irradiance

same simulation model, which analyses system performance. The PV power and MPPT power 9915 W have been measured and plotted in Figure 9a under various weather conditions. Figure 9b shows the boost converter voltage and current waveforms under several climate situations (422 V and 19.8, correspondingly).

5. HARDWARE IMPLEMENTATION

As illustrated in Figure 10a, the suggested scheme was constructed as a serviceable prototypical of a 10W PV

model and power converter. The suggested CNFF system has been connected to an Arduino Mega 2560, which allows duty cycle development based on input changes. Using a MATLAB simulation library, the Mega 2560 communicates directly with MATLAB. Table 2 contains design information. The suggested algorithm generates switching pulses, and its run cycle will alter when climate change occurs**.** Figure 10b shows how the suggested method generates half of the usage cycle. The suggested method generates a 90 percent operational cycle in Figure 10c. Figure 10e shows the suggested technique for the gate pulses under various climate circumstances in

MATLAB. Figure 10f shows a prototype model of a 28.20 V DC-DC converter with a 12 V input voltage.

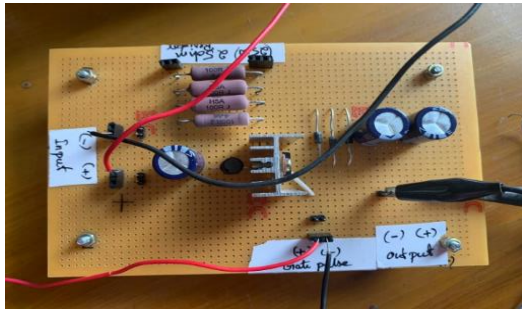**Figure 10a.** Working model of PV MPPT system
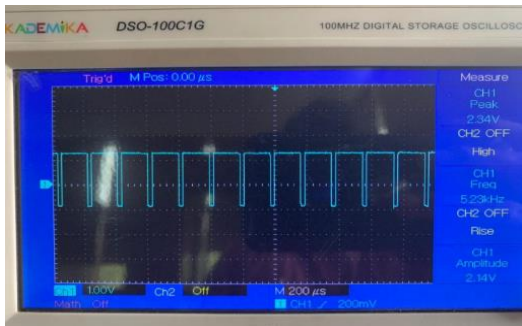

Figure 10b. DC-DC Converter Model

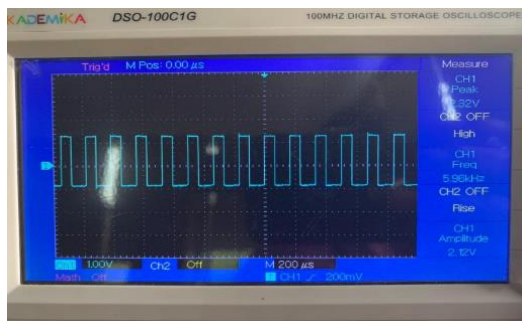**Figure 10c.** Switching signal with 50 % duty cycle

Figure 10d. Switching signal with 90 % duty cycle
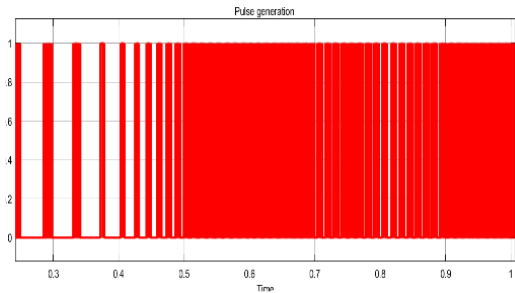
Figure 10e. Pulse generation by proposed CNFF algorithm
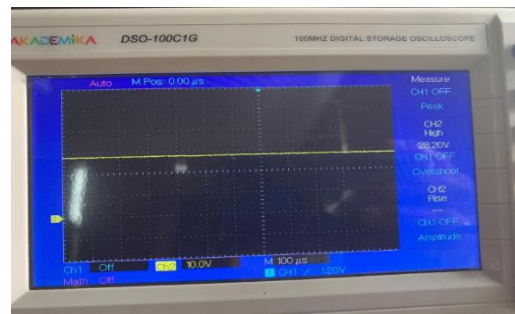
Figure 10f. DC-DC Converter Voltage 28.2 V for 12V of input

TABLE 1. Camparision table

S. No.	Name of algorithm	MPPT Power	Conversion Percentage
1	INC	8405	84.05%
2	P&O	9312	93.12%
3	Fuzzy	9773	97.73%
4	GA	9192	91.92%
5	PSO	9799	97.99%
6	CNFF	9915	99.15%

TABLE 2. Boost converter parameters

S. No.	Parameter	Value
1	Power	10W
2	Voc	21.20 V
3	Isc	0.66 A
4	Vmax	17.40 V
5	Imax	0.58 A
6	Capacitor C1	100 μf
7	Capacitor C2	4700 μf
8	Inductor	0.05 H
9	MOSFET	IRF540N
10	Resistance	33Ω

6. CONCLUSION

The maximum energy output of solar systems under a range of climatic circumstances was the focus of this study. The photovoltaic cell's mathematical model has been created, and its performance in various weather situations has been analyzed. As per the simulation findings, the MPPT process was required to produce the PV model maximum power. A number of MPPT processes were tried in this study under a range of climatological circumstances. The subsequent processes were analyzed, namely GA, PSO and CNFF. In comparison to other MPPT algorithms, The GA gives 91.92% of efficiency with 1.5s of time, The PSO MPPT gives maximum efficiency of 97.99% with 0.9s and finally the CFFNN delivers better outcomes like 99.15% of efficiency with 0.6 s of time according to simulation findings and comparative assessments. Finally, the suggested CFFNN MPPT algorithm was used to create and test prototype work model.

7. REFERENCES

1. M. Rupesh, T. S. Vishwanath "Comparative analysis of P & O and Incremental conductance methods for standalone PV system," *Internal Journal of Engineering and Technology*, Vol. 7, No. 3.29, (2018), 519-529. doi: 10.14419/ijet.v7i3.29.19303.

2. B. Hajipour, S.M Hasheminejad, H.R. Haghgou, "Extracting Technical Specifications of Solar Panel Type to design a 10 MW Hybrid Power Plant", *International Journal of Engineering, Transactions A: Basics*, Vol. 32, No. 4, April-2019, 562-568.doi: 10.5829/ije.2019.32.04a.14

3. M. Rupesh and T. V. Shivalingappa, "Evaluation of Optimum MPPT Technique for PV System using MATLAB/Simulink *International Journal of Engineering and Advanced Technology,* No. 5, (2019), 1403-1408.

4. H. Rahimi Mirazizi, M. Agha Shafiyi, "Evaluating Technical Requirements to Achieve Maximum Power Point in PV Powered Z-Source Inverter", *International Journal of Engineering, Transactions C, Aspects*, Vol. 31, No. 6, (2018), 921-931. doi: 10.5829/ije.2018.31.06c.09

5. L. Yang and Z. Yunbo, "A Novel Improved Variable Step Size INC MPPT Method for PV Systems", Chinese Control and Decision Conference (CCDC), Nanchang, China. (2019), 5070-5073, doi: 10.1109/CCDC.2019.8832451

6. D. Singh and H. Singh "Technical Survey and Review on MPPT Techniques to attain Maxim Power of Photovoltaic System", 5th International Conference on Signal Processing Computing and Control (ISPCC), Solan, India, (2019), 265-268, doi: 10.1109/ISPCC48220.2019.8988382

7. M. L. Azad, P. K. Sadhu and S. Das, "Comparative Study between P & O and Incremental Conduction MPPT Techniqus - A Review", International Conference on Intelligent Engineering and Management (ICIEM), Landon, UK, (2020), 217-222, doi: 10.1109/ICIEM48762.2020.9160316

8. M. Sarvi, M. Derakhshan, M. Sedighizadeh, "A New Intelligent Controller for Parallel DC/DC Converters", *International Journal of Engineering, Transactions A: Basics*, Vol. 27, No. 1, (2014), 131-142. doi: 10.5829/idosi.ije.2014.27.01a.16

9. D. Haji and N. Genc "Fuzzy and P & O based MPPT Controllers under different Conditions" 7th International Conference on Renewable Energy Research and Applications (ICRERA) Paris, France, (2018), 649-655, doi: 10.1109/ICRERA.2018.8566943.

10. M. L. Shah, A. Dhaneria, P. S. Modi, H. Khambhadia and K K D, "Fuzzy Logic MPPT for Grid Tie Solar Inverter", IEEE International Conference for Innovation in Technology (INOCON), Bangalore, India, (2020), doi: 10.1109/INOCON50539.2020.9298323.

11. M. R. Javed, A. Waleed, U. S. Virk and S. Z. Ul Hassan, "Comparison of the Adaptive Neural-Fuzzy Interface System (ANFIS) based Solar Maximum Power Point Tracking (MPPT) with other Solar MPPT Methods". IEEE 23rd International Multitopic Conference (INMIC) Bahawalpur, Pakistan, (2020), doi: 10.1109/INMIC50486.2020.9318178

12. T. Boutabba, S. Drid, L. Chrifi-Alaoui, M E Benbouzid, "A New Implementation of Maximum power Point Tracking based on Fuzzy Logic Algorithm for Solar Photovoltaic System", *International Journal of Engineering, Transactions A: Basics*, Vol. 31, No. 4, (2018), 580-587. doi: 10.58229/ije.2018.31.04a.09

13. H. Heidari, M Tarafdar Hagh, "Optimal Reconfiguration of Solar Photovoltaic Array using a Fast Parallelized Particle Swarm Optimization in Confront of Partial Shading", *International Journal of Engineering, Transaction B: Applications,* Vol. 32, No. 8, (2019), 1177-1185. doi: 10.5829/IJE.2019.32.08B.14

14. S Paul and J Thomas, "Comparison of MPPT using GA optimized ANN employing PI Controller for Solar PV system with MPPT using Incremental Conductance", International Conference on Power Signal Control and Computations (EPSCICON), Thrissur, India, (2014). doi: 10.1109/EPSCICON.2014.6887518

15. A Guediri, A. Guediri, S.Touil, "Optimization Using a Genetic algorithm based on DFIG Power Supply for the Electrical Grid", *International Journal of Engineering: Transaction A: Basics* Vol. 35, No. 1, (2022), 121-129. doi: 10.5829/IJE.2022.35.01A.11

16. L. Zaghba, M. Khennane, A. Borni, A. Fezzani, A.Bouchakour, Idriss Hadj Mahammed, Samir Hamid Oudjana "A Genetic Algorithm based improved P & O–PI MPPT Controller for stationery and Tracking Grid Connected Photovoltaic System", 7th International Renewable and Sustainable Energy Conference (IRSEC), Agadir, Morocco, (2019), 1-6. doi: 10.1109/IRSEC48032.2019.9078304

17. S. Paul, "Comparison of MPPT using GA Optimized ANN employed PI Controller with GA Optimized ANN employing fuzzy controller for PV System", IET 4th International Conference on Sustainable Energy and Intelligent Systems (SEISCON) Chennai, (2013), 266-271, doi: 10.1049/ic.2013.0324

18. R. Khanaki, M. A. M. Radzi, and M. H. Marhaban, "Comparison of ANN and P & O MPPT Methods for PV Applications under changing solar irradiance", IEEE Conference on Clean Energy and Technology (CEAT), Langkawi, Malasiya, (2013), 287-292, doi: 10.1109/CEAT.2013.6775642

19. H. Elaissaoui, M. Zerouali, A. E. Ougli and B. Thidaf, "MPPT Algorithm based on Fuzzy Logic and Artificial Neural Network (ANN) for a Hybrid Solar/Wind Power Generation System", 4th International Conference on Intelligent Computing in Data Sciences (ICDS), FEZ, Morocco, (2020), doi: 10.1109/ICDS50568.2020.9268747

20. M. S. Bouakkaz, A. Boukadoum, O. Boudebbouz, A. Bouraiou, N. boutasseta and I. Attoui, "ANN based MPPT Algorithm Design using Real Operating Climatic Condition", 2nd International Conference on Mathematics and Information Technology (ICMIT), Adrar, Algeria, (2020), 159-163, doi: 10.1109/ICMIT47780.2020.9046972

21. L. Bouselham, M. Hajji, B. Hajji and H Bouali, "A MPPT based ANN Controller applied to PV Pumping System", International Renewable and Sustainable Energy Conference (IRSEC), Marrakech, Morocco, (2016), 86-92, doi: 10.1109/IRSEC.2016.7983918

22. S. Messalti, A. G. Harrag and A E Loukriz, "A New Neural Networks MPPT Controller for PV Systems, IREC2015, the sixth" International Renewable Energy Congress, Sousse, Tunisia, (2015), doi: 10.1109/IREC.2015.7110907

23. Arulmozhiyal and K. R. Baskaran, "Implementation of a Fuzzy PI Controller for Speed Control of Induction Motors Using FPGA,"

Journal of Power Electronics, Vol. 10, (2010), 65-71, doi: 10.6113/JPE.2010.10.1.065

24. Sabir Messalti, D. Zhang, Abd Elhamid Loukriz., "Common Mode Circulating Current Control of Interleaved Three-Phase Two-Level Voltage-Source Converters with Discontinuous Space-Vector Modulation," IEEE Energy Conversion Congress and Exposition, Vol. 1-6, (2009), 3906-3912, doi: 10.1109/IREC.2015.7110907

25. Z. Yinhai, Songsong Wang, Haixia Xia, Jinfa Ge., "A Novel SVPWM Modulation Scheme," in Applied Power Electronics Conference and Exposition. APEC 2009. Twenty-Fourth Annual IEEE, (2009), 128-131. doi: 10.1109/APEC.2009.4802644.

Persian Abstract

چکیده

این تحقیق به چگونگی تولید انرژی سلول های فتوولتائیک (PV)در شرایط آب و هوایی مختلف می پردازد. برق فتوولتائیک امروزه نقش کلیدی در تولید انرژی و رفع نیازهای مصرف کنندگان در سراسر جهان ایفا می کند. توانایی سلول PV برای تولید الکتریسیته کاملاً به نور خورشید و نوسانات دما در محیط بستگی دارد. چندین محقق بر روی انواع روش های MPPT برای یک سیستم فتوولتائیک کار می کنند. تکنیک های قدیمی MPPT قادر به مقاومت در برابر تغییرات چشمگیر در شرایط آب و هوایی نیستند. هدف اساسی این مطالعه، ارتباط کنترل‌کننده‌های متعدد غیرماجراجویی و هوشمندانه برای MPPT سیستم PV، مانند PSO، GA، و CNFF است. محیط MATLAB برای ایجاد و شبیه سازی کنترل کننده هوشمند توصیه شده برای MPPT در سیستم PV استفاده شد. علاوه بر این، یافته‌های فوق‌الذکر مانند ولتاژ، جریان و توان با توجه به تابش و دمای مختلف مقایسه و ارزیابی می‌شوند. عملکرد توپولوژی های ذکر شده در بالا به کنترل کننده هوشمند بهینه برای سیستم PV مربوط می شود و نتیجه می گیرد که CFFNN با حداقل زمان لازم برای استخراج کارایی بهتری ارائه می دهد.